A central peaks as a pre-melting feature in $NaNO_3$ spectra

1990 J. Phys.: Condens. Matter 2 9125

(http://iopscience.iop.org/0953-8984/2/46/012)

J. Phys.: Condens. Matter **2** (1990) 9125–9131. Printed in the UK

A central peak as a pre-melting feature in $NaNO_3$ spectra

M D Fontana†, F Brehat‡ and B Wyncke‡

† CLOES, Supelec, and Université de Metz, 2 rue E Belin F-57078, Metz Cédex 3, France

‡ Laboratoire d'Infrarouge Lointain (Unité associée au CNRS 806), Université de Nancy I, BP 239, F-54506 Vandoeuvre, France

Received 16 February 1990, in final form 17 July 1990

Abstract. The quasi-elastic and Raman spectra of $NaNO_3$ are studied as a function of scattering configuration and temperature through the phase transition up to the close vicinity of the melting temperature. Results reveal the appearance of broad intense quasi-elastic scattering in the (ZZ) and (YX) spectra when the transition is approached from below. The slightly soft-phonon E_g lines detected in the (YZ) spectrum in the low-temperature phase are shown to persist above T_c. Neither the central peak, nor the phonon E_g modes seem to be connected with the transition to the high-temperature phase which is only partly disordered. Rather, the relaxational central peak is found to be related to the disordering process precursor of the melting.

1. Introduction

At room temperature, sodium nitrate ($NaNO_3$) crystals have a calcite structure (space group D_{3d}^6) with two formula units per unit cell. At around 275 °C the crystal undergoes a transition to a phase of D_{3d}^5 symmetry with one formula unit per primitive cell. This phase transition has been investigated by x-ray scattering (Terauchi and Yamada 1972), Raman scattering (see, e.g., Shen *et al* 1975, Neumann and Vogt 1978), infrared spectroscopy (Brehat and Wyncke 1985) and neutron diffraction (see, e.g., Lefebvre *et al* 1984). This phase transition was generally interpreted as due to an orientational disorder of the NO_3^- ions along the threefold c axis. Below T_c the nitrate groups have two antiparallel stable positions in the unit cell while above T_c they are randomly distributed between both positions. Nevertheless some questions concerning the dynamical mechanism remain open despite numerous investigations. In particular, Raman results contradict each other (compare Prasad Rao *et al* 1973, Shen *et al* 1975, Neumann and Vogt 1978). Further, a supplementary relaxation mode was needed to fit infrared spectra at low frequencies (Wyncke *et al* 1985). The associated relaxation time was found to exhibit an unexpected behaviour as a function of temperature since it continuously increases through the phase transition. Recently, several studies have been reported involving birefringence (Poon and Salje 1988) and spontaneous strain measurements (Reeder *et al* 1988) as well as molecular dynamics simulations (Lynden-Bell *et al* 1989). They are indicative of the current interest in the mechanism of the phase transition in $NaNO_3$.

0953-8984/90/469125 + 07 $03.50

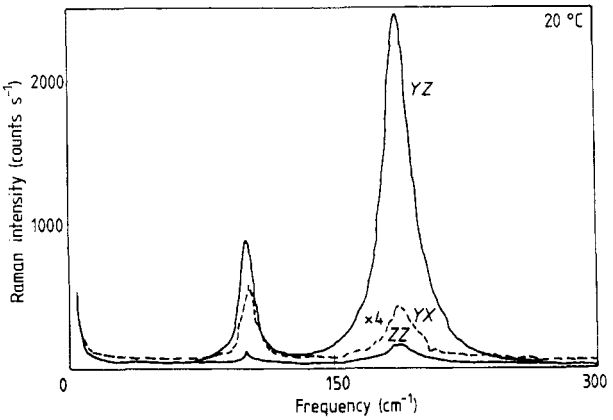

Figure 1. Raman spectrum of $NaNO_3$ at room temperature (20 °C) for several scattering configurations.

Our investigations concern low-frequency Raman scattering measurements in $NaNO_3$ crystals as a function of temperature, especially around the phase transition. Particular attention is paid to a careful quantitative analysis of the light polarization dependence which is reported for the first time for $NaNO_3$.

2. Experimental results

Raman scattering spectra have been carried out with a Spex double monochromator using the 514.5 nm exciting line of an Ar-ion laser. Measurements were made as a function of temperature from room temperature up to 290 °C, just above T_c and below the melting point (310 °C). Four right-angle scattering configurations were used, i.e. $X(ZZ)Y$, $X(ZX)Y$, $X(YZ)Y$ and $X(YX)Y$ where the X, Y and Z axes refer to the trigonal axes.

Of the external lattice modes, only two doubly degenerate modes of E_g symmetry are Raman active. The corresponding polarizability tensors have the following forms:

$$E_g^{(1)}:\begin{vmatrix} a & . & . \\ . & -a & b \\ . & b & . \end{vmatrix} \qquad E_g^{(2)}:\begin{vmatrix} . & -a & -b \\ -a & . & . \\ -b & . & . \end{vmatrix}. \tag{1}$$

The $X(YX)Y$, $X(ZX)Y$ and $X(YZ)Y$ configurations correspond to the observation of E_g symmetry modes while the $X(ZZ)Y$ geometry gives rise to only internal A_{1g} modes, which are located at a very high frequency. In order to achieve a quantitative comparison according to the scattering configurations, the spectra are recorded in exactly the same experimental conditions. For this, the laser beam goes through a quarter-wave plate and then a polarizer so that the incident light has the same intensity along the X and the Z axis, when propagating along the Y axis. In addition, the light scattered by the crystal is analysed and then circularly polarized before the spectrometer slit entrance.

Figure 1 shows the Raman spectra recorded in three configurations at room temperature. The (YZ) spectrum and the non-reported (ZX) spectrum appear to be very

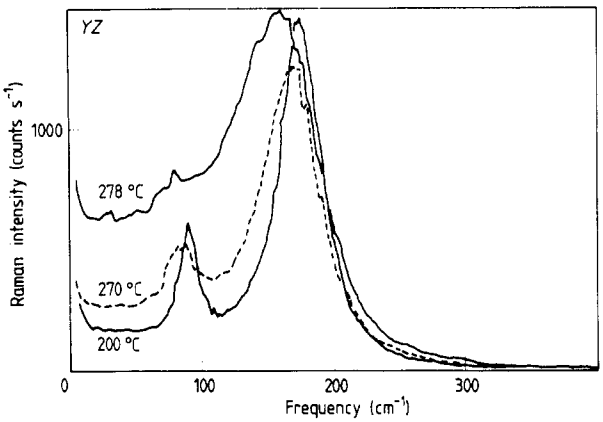

Figure 2. Raman spectrum of $NaNO_3$ recorded for the (YZ) geometry as a function of temperature.

similar to each other and display, at low frequencies, two well defined phonon lines of E_g symmetry at around 101 and 187 cm^{-1}. According to Nakagawa and Walter (1969) the first mode is due to the translational motion NO_3^- ions while the second mode corresponds to a librational motion of NO_3^- ions.

These modes are also observed in the $X(YX)Y$ scattering geometry but with an intensity much smaller than that of the $X(YZ)Y$ configuration. In addition, it is the lowest line which is the most intense in the (YX) geometry and not the second line. This may be attributed to the direct effect of the polarizability tensor (equation (1)). The (ZZ) spectrum exhibits two lines at the same location as in the (YZ) and (ZX) spectra, but with an intensity ten times less. Since no first-order external mode is required for the A_1 symmetry, both lines are in fact caused by contamination from the E_g symmetry due to a slight polarizer misorientation. Further, no extra line is detected in the (ZZ) spectrum, contrary to what was reported by Prasad Rao *et al* (1973). Figure 1 thus displays the clear effect of the light polarization on the Raman spectrum reported for the first time for $NaNO_3$ at room temperature.

The temperature dependence of the (YZ) spectrum is plotted in figure 2. A continuous shift downwards in frequency and an increase in linewidth are found for both E_g modes, as confirmed by calculations shown below. Similar behaviour is observed in the (ZX) spectrum. In the spectra a background intensity independent of frequency is superimposed on the normal E_g lines for temperatures above 200 °C. This background is found to increase slightly with increasing temperature. It can be interpreted as arising from a phonon density of states which is activated by increasing disorder in the low-temperature phase when the temperature is raised. This assumption is supported by specific heat measurements (Reinsborough and Wetmore 1967). It is corroborated by the large increase in the background at the transition, as shown in figure 2.

The behaviour of the (ZZ) spectrum as a function of temperature is illustrated in figure 3. Above 200 °C the spectrum exhibits the appearance of a broad quasi-elastic scattering which is superimposed upon the lines due to the E_g symmetry. The intensity of this central peak increases with increasing temperature so that the bands are completely obscured above 260 °C. This increase is particularly large when T_c (=275 °C) is approached from below and continues above T_c in the high-temperature phase. As

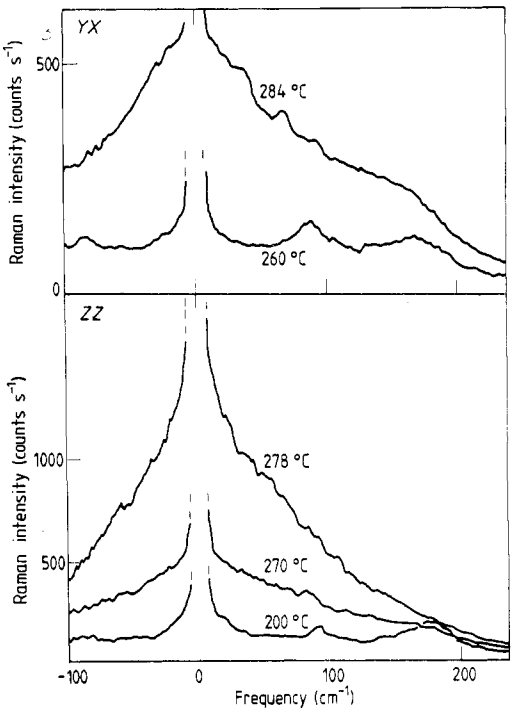

Figure 3. Temperature dependence of the low-frequency spectrum of $NaNO_3$ for the (YX) and (ZZ) polarizations.

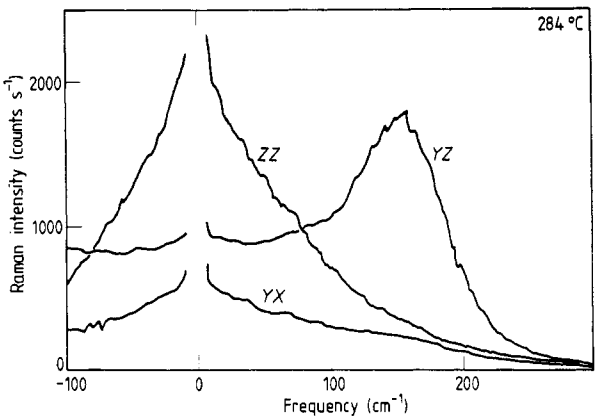

Figure 4. Light polarization dependence of the Raman spectrum for the high-temperature (284 °C) phase of $NaNO_3$. Note the change in comparison with figure 1.

shown in figure 3 a central mode also occurs in the (YX) spectrum besides the E_g lines but just above 260 °C, and with an intensity lower than in the (ZZ) spectrum. This seems to indicate that the origin of the central peak is different in the (ZZ) and (YX) spectra.

Figure 4 displays the spectra which are recorded above T_c in the same experimental conditions for the three main configurations. The (YZ) spectrum exhibits a broad intense phonon peak which is indicative of the persistence above T_c of the librational E_g mode. The (ZZ) and (YX) spectra are dominated at low frequencies by broad quasi-elastic

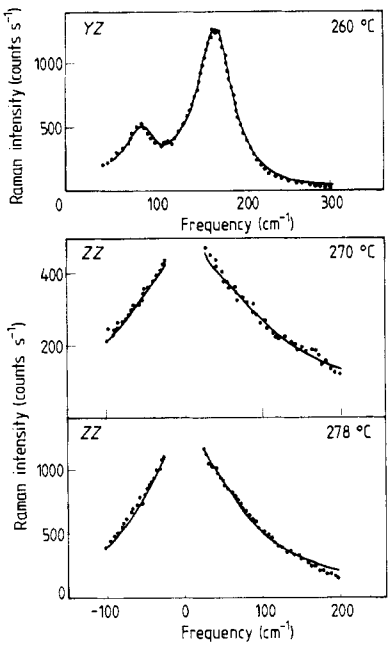

Figure 5. Typical (YZ) and (ZZ) spectra fitted with equations (2) and (3), respectively: ——, calculated spectra; ●, experimental data.

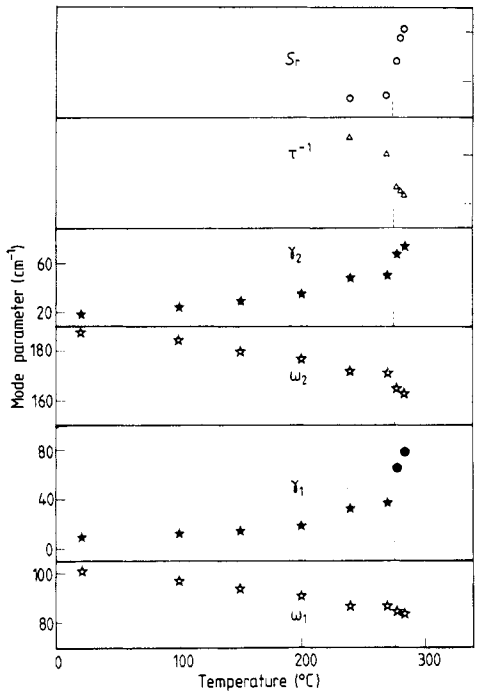

Figure 6. Temperature dependence of the parameters characterizing the E_g phonons and the central peak, as deduced from the fitting of the (YZ) spectrum with equation (2) and the (ZZ) spectrum with equation (3).

scattering, which is extended up to a very high frequency (about 250 cm^{-1}). The central peak intensity is shown to be much stronger in the (ZZ) spectrum. In the light of figures 3 and 4, it appears that

(i) the quasi-elastic scattering is really intrinsic and cannot be attributed to a Rayleigh line broadening and

(ii) it is anisotropic and not connected to the phase transition.

3. Analysis of the results

The E lines appearing in the (YZ) Raman spectra are fitted within the simple damped-harmonic oscillator model:

$$I(\omega) \propto S_1\omega\gamma_1/[(\omega_1^2 - \omega^2)^2 + \omega^2\gamma_1^2] + S_2\omega\gamma_2/[(\omega_2^2 - \omega^2)^2 + \omega^2\gamma_2^2] + a \qquad (2)$$

where S_j, ω_j, γ_j denote the strength, the frequency and the damping, respectively, for each mode and a is the temperature-dependent background intensity. Good agreement is achieved between experimental data and the spectrum deduced from equation (2) as shown in figure 5. The temperature dependence of the parameter values is reported in figure 6. Similar plots were previously given by Neumann and Vogt (1978). The frequency of each E_g mode continuously decreases on heating through T_c so that no E_g

mode disappearance is connected to the phase transition, contrary to what was claimed by Shen *et al* (1975). Further, a large increase in the damping constants γ_1 and γ_2 is found as the transition temperature is approached. The increase in damping is still strengthened above T_c, contrary to the usual damping behaviour expected for a mode related to a phase transition mechanism.

The (ZZ) spectrum is fitted assuming that the broad central scattered intensity is caused by a Debye relaxation mode:

$$I(\omega) \propto S_r \omega\tau/(1 + \omega^2\tau^2) \tag{3}$$

where τ is the relaxation time and S_r the relaxation strength. This form differs considerably from that used by Neumann and Vogt (1978) who have attributed the large scattering intensity to the superposition of the Rayleigh wing and the two damped phonon lines. The following are clearly seen in our spectra.

(i) The lines do not arise from normal modes but from contamination due to another symmetry. Furthermore the lines have a very weak intensity compared with the broad central peak above 260 °C.

(ii) The large scattering is only partly caused by the Rayleigh line which broadens when temperature increases. It is indeed possible to distinguish the diffuse scattering which is largely extended in frequency (up to 250 cm^{-1}) from a narrower Rayleigh scattering (see the spectrum at 270 °C in figure 3).

In the fitting of the (ZZ) spectrum with equation (3) the parameter S_r is used to attempt to reproduce the values of the dielectric permittivity ε along the z axis which was measured at 9 cm^{-1} (Wyncke *et al* 1985). Satisfactory agreement is obtained between experimental and calculated spectra as shown in figure 5. The behaviour of relaxation mode parameters is reported in figure 6. The parameter S_r exhibits a large increase in its value above T_c while the parameter τ^{-1} shows only slight changes in the low-temperature phase as well as in the high-temperature phase, with a drastic discontinuity at T_c (275 °C). The relaxation time displays relatively weak values (around 0.3×10^{-12} s below T_c and 0.5×10^{-12} s above T_c) compared with those deduced from the central peak detected by Raman spectroscopy in oxidic perovskites (Fontana *et al* 1985, 1988, 1990). This relaxation time is typically of the same order of magnitude as found in the other molecular disordered crystals such as alkali cyanides (Dultz 1976). The behaviour of the diffuse scattering as well as of the associated parameter S_r and τ show that it is not related to the phase transition occurring at around 275 °C. Only a large shift in the parameter values is noted at the transition.

Consequently the large central peak can be interpreted as a pre-melting phenomenon. This central peak may be therefore regarded as a feature induced by the disorder which is a precursor of the liquid state. This also explains the unexpected increase in the relaxation time through T_c, as deduced from infrared data (Wyncke *et al* 1985).

4. Conclusion

We have detected by Raman scattering measurements the occurrence of very intense quasi-elastic scattering which is extended to a very high frequency. This diffuse scattering intensity is very anisotropic and is shown to be strongest for the (ZZ) configuration. Neither E_g phonon lines nor the diffuse scattering seem to be related to the phase

transition mechanism at 275 °C. Further the central peak can be rather interpreted as due to a precursor feature of the melting.

The high-temperature phase is not completely disordered since the Raman spectrum still depends on the scattering configuration and displays persisting E_g lines of the ordered-low temperature phase.

The relaxation mode associated with this central peak in the (ZZ) spectrum may correspond to a motion of dipoles along the c axis while the central peak detected in the (YX) spectrum can be attributed to orientational fluctuations of the NO_3^- ions in the plane normal to the c axis.

References

Brehat F and Wyncke B 1985 *J. Phys. C: Solid State Phys.* **18** 4247
Dultz W 1976 *J. Chem. Phys.* **65** 2812
Fontana M D, Idrissi H and Wojcik K 1990 *Europhys. Lett.* **11** 419
Fontana M D, Kugel G E, Kania A and Roleder K 1985 *Japan J. Appl. Phys.* **24** suppl 24–2 516
Fontana M D, Ridah A, Kugel G E and Carabatos-Nedelec C 1988 *J. Phys. C: Solid State Phys.* **21** 5853
Lefebvre J, Fouret R and Zeyen C M E 1984 *J. Physique* **45** 1317
Lynden-Bell R M, Ferrario M, McDonald I R and Salje E 1989 *J. Phys.: Condens. Matter* **1** 6523
Nakagawa I and Walter J L 1969 *J. Chem. Phys.* **51** 1389
Neumann G and Vogt H 1978 *Phys. Status Solidi* b **85** 179
Poon W C K and Salje E 1988 *J. Phys. C: Solid State Phys.* **21** 715
Prasad Rao A D, Katiyar R S and Porto S P S 1973 *Advances in Raman Spectroscopy* ed J P Mathieu (London: Heyden) p 174
Reeder R J, Redfern S A T and Salje E 1988 *Phys. Chem. Minerals* **15** 605
Reinsborough V C and Wetmore F E W 1967 *Aust. J. Chem.* **20** 1
Shen T Y, Mitra S S, Prask H and Trevino S F 1975 *Phys. Rev.* B **12** 4530
Terauchi H and Yamada Y 1972 *J. Phys. Soc. Japan* **33** 446
Wyncke B, Brehat F and Kozlov G V 1985 *Phys. Status Solidi* b **129** 531